Biochimica et Biophysica Acta 1837 (2014) 98–111

Contents lists available at ScienceDirect

Biochimica et Biophysica Acta

journal homepage: www.elsevier.com/locate/bbabio

ROS generation and multiple forms of mammalian mitochondrial glycerol-3-phosphate dehydrogenase

Tomáš Mráček, Eliška Holzerová, Zdeněk Drahota, Nikola Kovářová, Marek Vrbacký, Pavel Ješina, Josef Houštěk *

Institute of Physiology Academy of Sciences of the Czech Republic v.v.i., Vídeňská 1083, 14220 Prague 4, Czech Republic

ARTICLE INFO

Article history:
Received 1 March 2013
Received in revised form 20 August 2013
Accepted 25 August 2013
Available online 30 August 2013

Keywords:
Mitochondrial glycerol-3-phosphate dehydrogenase
E.C. 1.1.5.3
ROS production
Supercomplex
In-gel ROS detection

ABSTRACT

Overproduction of reactive oxygen species (ROS) has been implicated in a range of pathologies. Mitochondrial flavin dehydrogenases glycerol-3-phosphate dehydrogenase (mGPDH) and succinate dehydrogenase (SDH) represent important ROS source, but the mechanism of electron leak is still poorly understood. To investigate the ROS production by the isolated dehydrogenases, we used brown adipose tissue mitochondria solubilized by digitonin as a model. Enzyme activity measurements and hydrogen peroxide production studies by Amplex Red fluorescence, and luminol luminescence in combination with oxygraphy revealed flavin as the most likely source of electron leak in SDH under in vivo conditions, while we propose coenzyme Q as the site of ROS production in the case of mGPDH. Distinct mechanism of ROS production by the two dehydrogenases is also apparent from induction of ROS generation by ferricyanide which is unique for mGPDH. Furthermore, using native electrophoretic systems, we demonstrated that mGPDH associates into homooligomers as well as high molecular weight supercomplexes, which represent native forms of mGPDH in the membrane. By this approach, we also directly demonstrated that isolated mGPDH itself as well as its supramolecular assemblies are all capable of ROS production.

1. Introduction

Reactive oxygen species (ROS) are produced by all eukaryotic cells and the predominant source in most of them is mitochondrial respiration [1]. ROS have been implicated to be instrumental in many pathological processes, ranging from oxidative phosphorylation (OXPHOS) dysfunction to chronic neurodegenerative diseases and cancer. In addition and partially in contrary to this detrimental role, ROS have also been proposed to function as signaling and regulatory factors in various metabolic processes [2].

Mitochondrial respiratory chain contains many components that may leak electrons. Since the pivotal experiments of Britton Chance [3,4], two major superoxide producing sites in mitochondria have been established: respiratory chain complex I (NADH:ubiquinone oxidoreductase) [5] and complex III (ubiquinol:cytochrome *c* oxidoreductase) [6]. In addition, several other components of mitochondrial respiratory chain have been proposed as potential sources of ROS. To date, at least four additional sites of superoxide production in mammalian mitochondria have been described. These sites include dihydrolipoamide dehydrogenase (component of α-ketoglutarate dehydrogenase and pyruvate dehydrogenase) [7,8], electron transferring flavoprotein (ETF):Q oxidoreductase [9,10], succinate dehydrogenase (SDH, complex II) [11], and mitochondrial glycerol-3-phosphate dehydrogenase (mGPDH) [12,13].

All of these enzymes are flavin dependent dehydrogenases functioning either in tricarboxylic acid metabolism or supplying electrons to coenzyme Q (CoQ) in the respiratory chain. mGPDH and SDH seem to play prominent roles in ROS production. Several studies have shown mGPDH to be a potent ROS producer both in mammalian and insect mitochondria [12,14]. Levels of ROS production from mGPDH can be very high, even comparable with the levels of ROS from Q_o site of complex III when inhibited with antimycin A (AA), i.e. the most potent ROS source in mitochondria [15]. Furthermore, a significant glycerol-3-phosphate (GP)-dependent ROS production has been found even in mitochondria from tissues with low mGPDH content. Here the amount of ROS produced per unit of mGPDH enzyme activity tends to be extremely high [16], although a significant portion of these ROS originates from flavin site of complex II [17]. mGPDH can therefore be a potentially important ROS source even in typically aerobic tissues with negligible enzyme content such as the heart [16].

On the contrary, SDH was considered to be well protected against electron leak and SDH associated ROS production was only linked to pathologies, where mutations in SDH subunits lead to defective

Abbreviations: AA, antimycin A; BAT, brown adipose tissue; CoQ, coenzyme Q; DCPIP, 2,6-dichlorophenolindophenol; FeCN, ferricyanide, potassium hexacyanoferrate(III); GP, sn-glycerol-3-phosphate; mGPDH, mitochondrial FAD-dependent glycerol-3-phosphate dehydrogenase; HAR, hexaammineruthenium(III) chloride; HQNO, 2-n-heptyl-4-hydroxyquinoline N-oxide; HRP, horseradish peroxidase; MXT, myxothiazol; OXPHOS, oxidative phosphorylation; ROS, reactive oxygen species; SDH, succinate dehydrogenase

* Corresponding author. Tel.: +420 241 062 434; fax: +420 241 062 149.
E-mail address: houstek@biomed.cas.cz (J. Houštěk).

0005-2728/$ – see front matter © 2013 Elsevier B.V. All rights reserved.
http://dx.doi.org/10.1016/j.bbabio.2013.08.007

coordination of prosthetic groups and subsequent leak of electrons [18]. However, it has been demonstrated very recently, that also SDH can produce significant amounts of ROS when levels of available succinate are low. Here flavin was implicated as the ROS source — under low succinate concentrations, flavin site is not fully occupied by the substrate and may therefore be accessible to oxygen, allowing electron leak and superoxide formation [11]. In vivo steady state concentrations of succinate have been reported to be approximately 0.5 mM in the tissues [19] or even in the micromolar range for cells in tissue culture [20,21]. Such mode of ROS production by SDH may therefore be a significant contributor to the overall cellular ROS levels.

Despite these recent advances in understanding of flavin dehydrogenases dependent ROS production, detailed molecular mechanism of electron leak is still missing and may differ between individual enzymes. For example the mechanism of ROS production by mGPDH has been shown to be in many respects different from ROS production at other sites of the respiratory chain: (i) mGPDH has a simple structure and is localized on the outer side of the inner mitochondrial membrane but despite that, ROS are produced equally to both sides of the membrane [14]; (ii) it displays unique and specific activation of electron leak by ferricyanide [12,15,22]; (iii) its expression is highly tissue dependent and mGPDH may be a significant contributor to overall ROS production in glycolytic tissues [13]. All this stresses out the importance to further characterize pathways leading to electron leak in flavin dehydrogenases.

Over the last couple of years our understanding of inner mitochondrial membrane organization changed significantly as theory of respiratory chain supercomplexes gained traction. OXPHOS supercomplexes were proposed to play several roles — apart from facilitation of their biogenesis, supercomplex organization should improve substrate channeling between individual complexes and thus reduce the chance of electron leak and ROS production. So far, such type of association has clearly been documented only for complex I, but given the potential for electron leak from SDH and mGPDH their protection by streamlining the electron transport by association into supercomplex would make thermodynamic sense. However, so far there are only limited data on supramolecular organization of these enzymes. For example, in bacteria it is documented that SDH forms trimers, which are the active conformation [23] but no data on association with other OXPHOS complexes are available. In case of mGPDH, in yeast it has been shown that several mitochondrial dehydrogenases including mGPDH analog Gut2p associate into supramolecular complex but again without clear further association with downstream OXPHOS complexes [24].

In this study we focused on mGPDH and SDH and their ability to support ROS formation at different sites of respiratory chain. We used mild detergent digitonin to solubilize mitochondrial membranes into individual complexes and supercomplexes of respiratory chain enzymes as a tool for elucidating their role in ROS production. Mild detergent solubilization also allowed us to study native organization of these dehydrogenases in the inner mitochondrial membrane and formation of higher molecular weight complexes.

2. Material and methods

2.1. Isolation of mitochondria and solubilization

For experiments we used interscapular brown adipose tissue (BAT) of one to three weeks old Wistar rats kept at room temperature and 12 h/12 h light/dark cycle on a standard diet and water supply ad libitum. All animal works were approved by the institutional ethics committee and were in accordance with the EU Directive 2010/63/EU for animal experiments. Mitochondria were isolated in STE medium (250 mM sucrose, 10 mM Tris–HCl, 1 mM EDTA, pH 7.4) supplemented with BSA (10 mg.mL^{-1}) by differential centrifugation [25] and frozen at −80 °C. Subsequently frozen–thawed mitochondria were used in experiments. Membrane proteins were solubilized in KCl based medium (120 mM KCl, 3 mM HEPES, 5 mM KH_2PO_4, 3 mM $MgSO_4$, 1 mM EGTA, pH 7.2) with varying amount of digitonin (1 to 8 w/w ratio detergent/protein) for 10 min on ice and separated into supernatant and sediment fraction by centrifugation 20 min at 20,000 *g*.

2.2. Enzyme activity assays

Activities of SDH and mGPDH were determined spectrophotometrically either as CoQ_1 (monitored at 275 nm, $\varepsilon_{275} = 13.6$ mM^{-1}.cm^{-1}), 2,6-dichlorophenolindophenol (DCPIP, monitored at 610 nm, $\varepsilon_{610} = 20.1$ mM^{-1}.cm^{-1}) or cytochrome *c* oxidoreductases (monitored at 550 nm, $\varepsilon_{550} = 19.6$ mM^{-1}.cm^{-1}). The assay medium contained 50 mM KCl, 10 mM Tris–HCl, 1 mM EDTA, 1 mg.mL^{-1} BSA, 1 mM KCN, pH 7.4 and 25 μM CoQ_1, 10 mM 2,6-dichlorophenolindophenol (DCPIP) or 50 μM cytochrome *c* respectively. The reaction was started by adding 10 mM sn-glycerol -3-phosphate (GP) or succinate and changes of absorbance were monitored at 30 °C. Enzyme activities were expressed as nmol.min^{-1}.mg^{-1} protein.

2.3. Fluorometric detection of hydrogen peroxide production

Hydrogen peroxide production was determined fluorometrically by measuring oxidation of Amplex Red coupled to the enzymatic reduction of H_2O_2 by horseradish peroxidase (HRP). Fluorescence of the Amplex Red oxidation product was measured at 37 °C using Tecan Infinite M200 multiwell fluorometer. Excitation/emission wavelengths were 544 nm (bandwidth 15 nm)/590 nm (bandwidth 30 nm). The assay was performed with 15 μg of mitochondrial protein per mL in KCl based medium (120 mM KCl, 3 mM HEPES, 5 mM KH_2PO_4, 3 mM $MgSO_4$, 1 mM EGTA, pH 7.2) supplemented either with 10 mM succinate or 10 mM GP. Amplex Red was used at the final concentration of 50 μM with HRP at 1 U.mL^{-1}. Where indicated, 1 μg.mL^{-1} antimycin A (AA) or 12 μM CoQ_1 was added. Fluorescence signal from the well containing all substrates and inhibitors, but not mitochondria, was subtracted as background for every experimental condition used. Thus any non-enzymatic effect of inhibitors on apparent ROS production was eliminated. Signal was calibrated using H_2O_2 at the final concentration of 0–5 μM and H_2O_2 stock concentration was routinely checked by measuring its absorption at 240 nm.

2.4. ROS production in gel slices

Proteins in solubilizates were separated by hrCN3-PAGE [26] on 4–13% gradient gels. Individual lanes were excised and washed 3 × 10 min in KCl based medium (120 mM KCl, 3 mM HEPES, 5 mM KH_2PO_4, 3 mM $MgSO_4$, 1 mM EGTA, pH 7.2) to remove salts used in electrophoresis buffers. Subsequently, each lane was cut to 1 mm long slices by custom made cutter. Individual slices (circa 1 × 1 × 6 mm) were transferred into separate wells of 96 well plate and ROS production was detected by Amplex Red dye using the same conditions as for solubilized mitochondria (see above). Four measurements were done for each well (Tecan reader always uses only part of the well area for fluorescence detection) to ensure that presence of gel slice did not cause inhomogeneity and average was used in calculations. In-well SD was within 10%, which was the same as with mitochondria or solubilizates. As we do not know exact protein content in each slice, values were only expressed as pmol H_2O_2.min^{-1}.

2.5. Luminescence detection of hydrogen peroxide production

ROS production was also measured as luminescence, principally as described earlier [27]. Tecan Infinite M200 in luminescence mode was used to detect signal. Measurements were performed at 37 °C in 0.1 mL of KCl based medium, as in Amplex Red assay (120 mM KCl, 3 mM HEPES, 5 mM KH_2PO_4, 3 mM $MgSO_4$, 1 mM EGTA, pH 7.2) containing 1 μM myxothiazol (MXT), 1 mM luminol (5-amino-2,3-dihydro-1,4-

phtalazinedione) and 2.5 U.mL^{-1} HRP. 10 μg of solubilizate (digitonin 2 g/g) protein was used per well. Assay was performed on per well basis — the reaction was started by 10 mM GP or succinate, after 60 s 500 μM ferricyanide (potassium hexacyanoferrate(III); FeCN) was added. Other conditions are specified in Results and Legends to figures. Luminescence was recorded in 0.5 s intervals for further 60 s. The luminescence peak reached maximum values in the first second after FeCN injection and declined subsequently. For evaluation of peroxide production the maximum value (peak) was used. This value was proportional to integral luminescence intensity over the whole 60 second period. Each trace represents average value of quadruplicate measurement done in series. A calibration with hydrogen peroxide was routinely performed to check for the linearity of response.

2.6. Western blotting

Proteins in solubilizates were analyzed by BN-PAGE and hrCN3-PAGE [26,28] on 4–13% separating gels using the Mini-Protean III apparatus (BioRad). For two-dimensional electrophoresis, gel slices from the 1st dimension were incubated in 1% SDS and 1% mercaptoethanol for 1 h and then subjected to SDS-PAGE on 10% gels [29]. Proteins were transferred from gels to PVDF-membranes (Immobilon-P, Millipore) using semidry electrotransfer (BioRad). The membranes were blocked with 5% non-fat dried milk in TBST (150 mM NaCl, 10 mM Tris, 0.1% Tween-20, pH 7.5) for 1 h and incubated for 2 h with the specific primary antibodies diluted in TBST. Monoclonal antibodies to SDHA and Blue Native OXPHOS Complexes Detection Kit (containing monoclonal antibodies to NDUFA9, SDHA, Core2, Cox4, α-subunit of complex V) were obtained from Abcam; rabbit polyclonal antibody to mGPDH was custom prepared [30]. Membranes were then incubated for 1 h with corresponding secondary fluorescent antibodies — IRDye 680- or 800-conjugated goat anti-mouse IgG (Invitrogen) or goat anti-rabbit IgG (Rockland). Detection of proteins was performed using Odyssey fluorescence scanner. The quantification of signals was carried out in Aida Image Analyzer program version 3.21.

2.7. In-gel activity staining of mGPDH

Activity staining of mGPDH in native gels was performed according to a modified protocol originally described in [31]. Gel slices were stained using solution of 5 mM Tris–HCl (pH 7.4), 3 mM $MgCl_2$, 0.88 mM menadione, 1.2 mM NitroBlue Tetrazolium, 1.5 μM rotenone, 2 μM KCN and 10 mM glycerol-3-phosphate for 1 h. Subsequently gels were denatured in 50% methanol/10% acetic acid for 15 min, fixed in 10% acetic acid for 10 min and scanned on flatbed scanner.

2.8. Polarographic detection of oxygen consumption

Oxygen consumption was measured at 30 °C as described before [12] using Oxygraph-2k (Oroboros, Austria). Measurements were performed in 2 mL of KCl medium (80 mM KCl, 10 mM Tris–HCl, 3 mM $MgCl_2$, 1 mM EDTA, 5 mM K-Pi, pH 7.4) using 50–100 μg protein.mL^{-1} of digitonin solubilized mitochondria. For measurements, 10 mM GP, 125 μM hexaammineruthenium(III)chloride (HAR), 62.5 μM FeCN, 16 μM CoQ_1, and 1 μM MXT were used. The oxygen consumption was expressed in pmol oxygen.s^{-1}.mg^{-1} protein.

3. Results

3.1. Solubilization of mitochondrial membrane with digitonin affects mGPDH and SDH enzyme activities by CoQ depletion

Solubilization of mitochondrial membrane using mild nonionic detergents represents established approach to obtain respiratory chain enzymes in a range of different forms, from monomers to supercomplexes depending on the type and concentration of the detergent used. To study mGPDH and SDH in a soluble state, BAT mitochondria were solubilized with increasing concentrations of digitonin (1–8 g/g protein) and the solubilized (supernatant) and the residual non-soluble (sediment) fractions were separated by the centrifugation (20,000 *g*, 20 min). The average amounts of the protein recovered in supernatants after solubilization were 51.5, 70.4, 82.8, 81.9 and 64.5% of the original mitochondrial protein at 1, 2, 4, 6 and 8 g digitonin/g protein, respectively. The composition of the fractions was analyzed by SDS-PAGE and WB. As shown in Supplementary Fig. 1, specific content of respiratory chain complexes was quantified using subunit specific antibodies. Within the range of detergent concentrations used, the relative content of respiratory chain complexes, including SDH and mGPDH was maintained at levels similar to the original mitochondria. To assess the effect of solubilization on these dehydrogenases, we compared the specific activities (activities expressed per mg of protein in each sample) of mGPDH and SDH in the whole, frozen thawed mitochondria and in detergent solubilized mitochondrial proteins, i.e. at conditions when the dehydrogenases as well as the whole OXPHOS are assembled in the membrane versus the conditions when the membrane structure and interaction with mobile carriers and other respiratory chain complexes are disrupted by membrane solubilization. We followed the sole activity of mGPDH and SDH using DCPIP or CoQ (DH:DCPIP, DH:Q) as the acceptor as well as the combined activity of dehydrogenase and complex III (GCCR, SCCR). Solubilization of mitochondria by digitonin caused pronounced decline of GCCR and SCCR activity with increasing detergent concentration (Fig. 1). However, samples solubilized with digitonin 1 g/g protein still retained up to 10 and 27% of GCCR and SCCR activity in the soluble fraction respectively i.e. indicating presence of functional respiratory patches composed of at least dehydrogenase and complex III under these mild conditions, while electron transport to cytochrome *c* was completely abolished at higher digitonin concentrations.

Observed decrease in the sole activities of both solubilized dehydrogenases (acceptors DCPIP or CoQ) that declined with increasing detergent concentration, was much less pronounced and occurred at higher detergent/protein ratios than was the case for GCCR or SCCR. When comparing two acceptors for isolated dehydrogenase activity, we observed faster decline of DH:DCPIP than DH:Q activity, which was even more pronounced in SDH than in mGPDH. As DCPIP does not take electrons directly from the dehydrogenases, but takes them preferentially via CoQ pool [32], this suggested that CoQ_9 is effectively depleted from the dehydrogenase containing micelles during digitonin solubilization. Therefore, we tested effect of exogenous CoQ_1 supplementation. Addition of exogenous CoQ_1 to digitonin 2 g/g protein solubilizates significantly increased measured activities for both dehydrogenases. The activating effect was much more pronounced in SDH (>20-fold increase) than in mGPDH (2-fold increase) (Fig. 2), in accordance with much higher decline and almost complete loss of succinate:DCPIP activities in the digitonin solubilizates. This translated to approximately 5-fold higher specific activity of SDH compared to that of mGPDH. On the one hand, this difference points to a significant inactivation of mGPDH during solubilization by nonionic detergents, a general problem previously observed in mGPDH isolation and purification [33]. On the other hand, it indicates that bound CoQ is more easily and efficiently lost from SDH than mGPDH, in accordance with minute content of CoQ observed in isolated SDH [34].

3.2. ROS production by digitonin solubilized mGPDH and SDH responds differently to external CoQ

To characterize ROS production by solubilized mGPDH and SDH, we measured GP- and succinate-induced hydrogen peroxide production at 10 mM substrate concentration following oxidation of 50 μM Amplex Red in the presence of added peroxidase (1 U.mL^{-1}). When dehydrogenase-dependent ROS production was analyzed as succinate-induced ROS production in mitochondria (Fig. 3B, "0" digitonin values), it showed very low basal levels (50 pmol H_2O_2.min^{-1}.mg^{-1} protein)

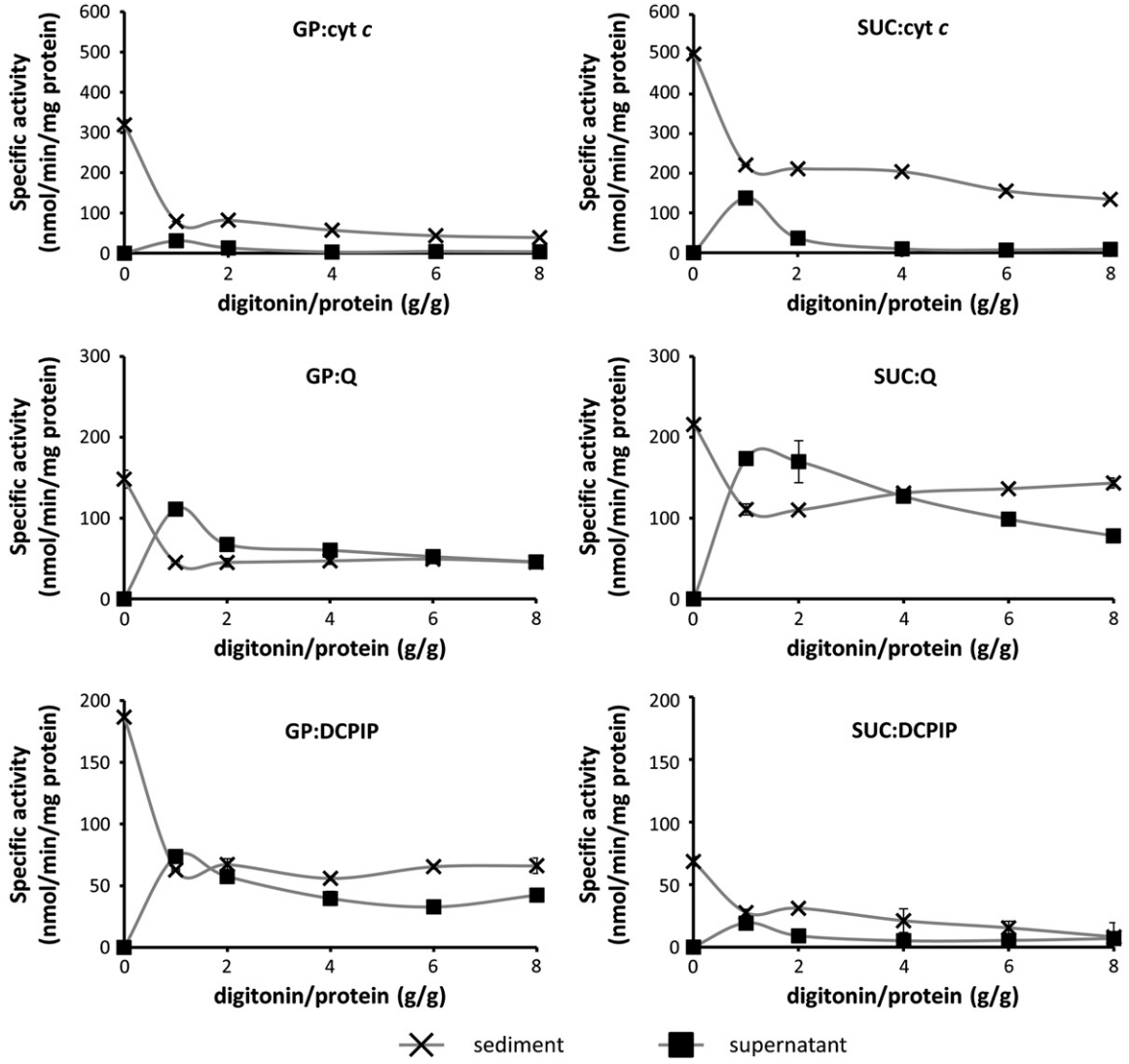

Fig. 1. Enzyme activities in digitonin-solubilized BAT mitochondria. Mitochondria were solubilized with increasing amounts of digitonin (1, 2, 4, 6, 8 g/g protein). SDH and mGPDH enzyme activities were detected both in supernatants and sediments (20,000 *g*) after solubilization. Activities were determined as CoQ_1 reductase (GP:Q, succinate:Q) or DCPIP reductase (GP:DCPIP, succinate:DCPIP), i.e. isolated dehydrogenase activity or as cytochrome *c* reductase (GP:cyt *c*, succinate:cyt *c*), i.e. combined activity of dehydrogenase and complex III, referring about intactness of electron transport chain in respective sample. Activities are expressed per mg protein of solubilizates (digitonin 1–8 g/g protein) or mitochondria (digitonin 0). Results are mean ± SD from 2 to 4 replicates.

but strong, more than 5-fold activation by myxothiazol (MXT). This effect of MXT on SDH-dependent ROS generation rapidly declined in solubilized enzyme with increasing digitonin concentration, analogically to SCCR and succinate:DCPIP activity (Fig. 1). In the case of mGPDH-dependent ROS production, the basal mitochondrial ROS production was higher (140 pmol $H_2O_2.min^{-1}.mg^{-1}$ protein) (Fig. 3A) and MXT displayed similar activation in whole mitochondria. But, in a sharp contrast to SDH, solubilization of the inner mitochondrial membrane led to the pronounced increase in basal mGPDH-dependent ROS production at increasing digitonin concentrations. Despite higher SCCR than GCCR activities in isolated mitochondria (see "0" digitonin values for supernatants in Fig. 1), mGPDH-dependent ROS production in fully solubilized mitochondrial membranes (digitonin 4–8 g/g protein) was >15 fold higher than SDH-dependent ROS production.

It has been recently reported, that SDH may be a significant ROS producer under low succinate concentrations [11]. We therefore determined the levels of ROS production with 0.4 mM succinate as well. As seen in Fig. 3C, the pattern of SDH-dependent ROS generation was rather different under these conditions. As in the case of 10 mM succinate, basal ROS production in mitochondria was low with 0.4 mM succinate and it was strongly increased by blockade of complex III by MXT. To the contrary, basal ROS production with 0.4 mM succinate concentration was strongly stimulated by detergent solubilization, steadily increasing up to the highest digitonin concentration used, similarly as was the case for mGPDH-dependent ROS production. With all substrates used, no activation effect of MXT was observed in solubilizates with digitonin 4–8 g/g protein respectively, indicating that at these detergent concentrations dehydrogenases do not communicate directly with complex III and the observed ROS production originates solely from the respective dehydrogenases. These data are in general agreement with dehydrogenase:cyt *c* enzyme activities measured in Fig. 1. It should also be noted that the actual absolute levels of ROS production with 0.4 mM succinate are underestimated, as SDH is known to be inhibited by oxaloacetate [35,36] and 0.4 mM succinate is not sufficient to displace oxaloacetate from the active site of the enzyme. As can be seen from Supplementary Fig. 2, approximately 50–60% of SDH in our preparations was in inactive state. While with 10 mM succinate, this inhibition is released and whole bulk of the enzyme contributes to the ROS production, for 0.4 mM succinate the inactivated portion of SDH does not contribute to the measured ROS production. However, this does not have effect on the relative changes in ROS production due to solubilization or inhibitor action.

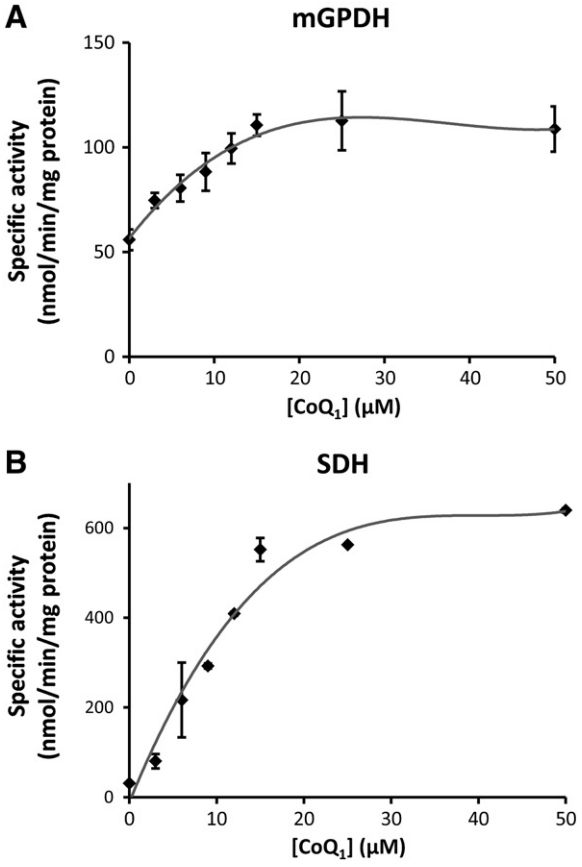

Fig. 2. Activation of digitonin-solubilized dehydrogenases by CoQ. Effect of CoQ_1 addition on mGPDH (A) and SDH (B) enzyme activities measured as dehydrogenase:DCPIP reductases was studied in BAT mitochondria solubilized with digitonin (2 g/g protein 20,000 *g* supernatants). 0 to 50 μM CoQ_1 was added to the cuvette and enzyme activity was measured. Results are mean ± SEM from 3 to 5 measurements.

Recent work of Brand's group [11] suggested significant portion of mGPDH-dependent ROS to originate from SDH due to reverse flow of electrons. This is possibly of lower importance in frozen thawed mitochondria used in our experiments, but as shown in Supplementary Fig. 3, in frozen mitochondria supplied with GP, there is still significant SDH-dependent portion of ROS under the conditions with MXT present (compare values with MXT vs. MXT + atpenin A5). However, this part of ROS production is completely abolished in solubilized mitochondria, where dehydrogenases cannot communicate directly via CoQ pool (Supplementary Fig. 3).

As mGPDH and SDH are supposed to differ in their ability to bind CoQ, we decided to analyze effect of exogenous CoQ_1 on the measured ROS production (data in Fig. 3D–F and in the redrawn form in Fig. 4 to emphasize differences between membrane-bound and solubilized dehydrogenases). Addition of oxidized CoQ_1 to isolated mitochondria had prooxidant effect for all three substrates tested: GP (Fig. 4A), succinate 10 mM (Fig. 4B) and succinate 0.4 mM (Fig. 4C). This prooxidant behavior of CoQ_1 was fully retained after addition of complex III inhibitor — MXT, while the absolute values of ROS production after MXT addition rose as in the absence of CoQ_1 (Fig. 4A–C). The effects of CoQ_1 and MXT were thus simply additive, probably reflecting the increase in available CoQ pool size. This behavior changed, when fully solubilized complexes (digitonin 6 g/g protein) were studied. Here CoQ_1 had strong antioxidant effect on ROS production with GP (Fig. 4D) and 0.4 mM succinate (Fig. 4F), while it still acted as prooxidant in case of 10 mM succinate (Fig. 4E). Addition of MXT alone to solubilized mitochondria did not influence basal ROS production, but it abolished antioxidant effect of CoQ_1 on GP and 0.4 mM succinate (Fig. 4D–F). In the case of 0.4 mM succinate, CoQ_1 and MXT led to even more pronounced ROS production than observed at basal levels (726 ± 31 vs. 266 ± 22 pmol.min^{-1}.mg^{-1}), representing the highest ROS production observed in solubilized mitochondria (Fig. 4E). Thus the ability to reoxidate soluble CoQ_1 on complex III (which is still present in the solubilizate, albeit not in the same respiratory supercomplex as flavin dehydrogenases) seems to be essential for its antioxidant effect on ROS production supported by GP and 0.4 mM succinate. Overall picture of pro-/anti-oxidant effects was the same when AA was used as complex III inhibitor. However, absolute ROS production with AA was higher given the fact, that ROS are under these conditions produced at the level of complex III as well (data not shown). Presumably loss of endogenous CoQ_9 facilitates electron leak from mGPDH, supporting the view that Q-binding site is the locus of electron leak. In case of SDH analogous mechanism seems to operate at low substrate concentration, probably reflecting the direct effect of CoQ on SDH activity [37], even though the substrate binding site was proposed to generate ROS at these conditions [11].

3.3. Electron leak induction by single electron acceptors

In further experiments we followed ROS production induced by single electron acceptor potassium ferricyanide (FeCN). Here, ROS production can be detected as a burst of oxygen consumption due to the formation of hydrogen peroxide under the conditions, when respiratory chain is blocked at the level of complex III (with AA or MXT) or complex IV (with KCN). This phenomenon has been demonstrated in mitochondria with GP but not with succinate used as a substrate [12]. Presumably, FeCN accepts one electron from mGPDH and the second electron leaks to oxygen, forming superoxide ($O_2^{\bullet -}$) which is subsequently dismutated to hydrogen peroxide. The net effect manifests as oxygen consumption, which can be abolished by the presence of catalase that induces decomposition of hydrogen peroxide to water and oxygen (not shown and [12]).

As shown in Fig. 5A, the FeCN-induced oxygen consumption by mGPDH is fully retained after solubilization with digitonin (2 g/g protein). Similarly to whole mitochondria [12], it is completely prevented by addition of CoQ_1 (Fig. 5A) or by addition of another one-electron acceptor, hexaammineruthenium(III) chloride (HAR) (Fig. 5B). Electron leak due to one electron transfer to FeCN can therefore be disturbed by other electron acceptors interacting with mGPDH, presumably downstream of the flavin site. Complex II inhibitor atpenin A5 did not influence GP-dependent, FeCN-induced electron leak (Fig. 5C), indicating that the leak occurs directly on mGPDH and not indirectly via electron backflow towards SDH. As in mitochondria, no FeCN-induced ROS production can be observed in digitonin (2 g/g protein) solubilizates with 10 mM succinate (not shown). However, as SDH was shown to produce ROS at much higher rate with low succinate concentrations, we tested FeCN effect with 0.4 mM succinate. Nevertheless, neither here there was any observable induction by FeCN of oxygen consumption due to electron leak (Fig. 5D). Leak of electrons from flavin in SDH may also be facilitated by blockade of CoQ binding site by atpenin A5. Here FeCN would allow for the electrons to be channeled away immediately upstream of atpenin binding site but neither the addition of atpenin induced FeCN-mediated leak with 0.4 mM succinate (Fig. 5D). To make sure that atpenin A5 acts as a specific SDH inhibitor even for solubilized enzymes, we followed the effect of atpenin A5 on mGPDH and SDH activities (Supplementary Fig. 4A–C). As can be seen, atpenin A5 did not inhibit mGPDH when measured either as Q, DCPIP or FeCN reductase, but fully inhibited succinate:Q and succinate:DCPIP activity and only partially abrogated succinate:FeCN activity, which is in agreement with atpenin A5's role as specific SDH inhibitor acting at CoQ binding site. This points to a major difference between mGPDH and SDH in the mechanism of electron leak and ROS generation.

Broad absorption spectrum of FeCN interferes with the fluorescent detection of oxidized Amplex Red, but FeCN-induced ROS production

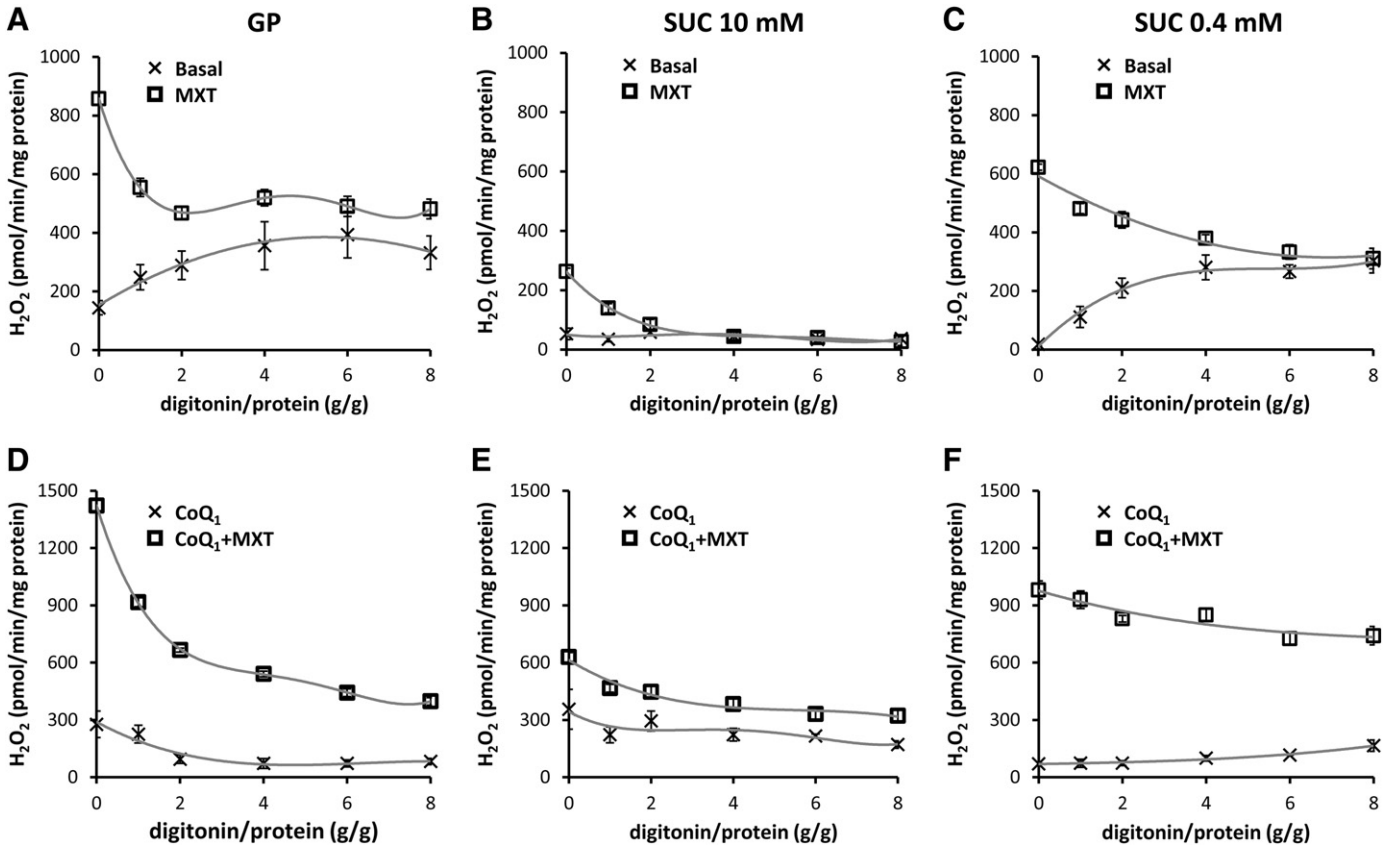

Fig. 3. Reactive oxygen species production in digitonin-solubilized BAT mitochondria. Mitochondria were solubilized with increasing amounts of digitonin (1, 2, 4, 6, 8 g/g protein) and ROS were detected as hydrogen peroxide production measured fluorometrically following oxidation of Amplex Red (50 μM) in the presence of HRP (1 $U.mL^{-1}$) in mitochondria (0 digitonin values) and 20,000 *g* supernatants after digitonin solubilization. 10 mM glycerol-3-phosphate (GP), 10 mM succinate (SUC 10 mM) or 0.4 mM succinate (SUC 0.4 mM) was used as substrate respectively. Titration curves are for basal ROS production without inhibitor (Basal), in the presence of 1 μM myxothiazol (MXT), 12 μM CoQ_1 (CoQ_1) or 12 μM CoQ_1 plus 1 μM myxothiazol (CoQ1 + MXT). Note that effect of myxothiazol, inhibitor of complex III, on ROS production can only be observed in mitochondria and at low digitonin/protein ratios, when intact electron transfer pathway between dehydrogenase and complex III exists. Results are mean ± SD from 3 to 6 replicates.

can also be detected by luminometry [12]. Here, HRP mediated luminol oxidation causes luminescence flash and is detected. As can be seen in Fig. 6A, FeCN can induce GP-dependent electron leak in digitonin 2 g/g protein solubilizates, while there is no observable electron leak with HAR under the same conditions. HAR also partially inhibits FeCN-induced electron leak (Fig. 6B and D), both when added after the FeCN (Fig. 6B) or when prior present in the medium (Fig. 6D). These data are in accordance with the analogous measurements of oxygen consumption (Fig. 5B). We cannot confirm that HAR accepts electron directly from the dehydrogenase, as HAR redox state cannot be detected spectrophotometrically. Nevertheless, from Supplementary Fig. 4D it is obvious, that HAR can positively influence apparent rate of FeCN reduction in spectrophotometric activity assay, indicating that HAR can facilitate electron transfer to FeCN, possibly as an intermediate electron carrier. Further, we wanted to confirm that mGPDH electron leak really occurs on the dehydrogenase itself. Fig. 6C demonstrates significant FeCN-induced ROS production in digitonin 2 g/g protein solubilizates with GP as a substrate in the presence of 1 μM rotenone, 1 μM MXT, 1 $mg.mL^{-1}$ AA, 1 μM atpenin A5 and 10 mM malonate, it is at conditions when all other possible sites of electron leak have been blocked by their respective inhibitors. Maximum luminescence peak in the presence of all inhibitors was only marginally changed compared to basal conditions, thus demonstrating that in overall ROS production the primary source of FeCN-mediated electron leak has to be mGPDH. There was also no significant ROS production when sn-glycerol-2-phosphate, a glycerol-3-phosphate stereoisomer that is not oxidized by mGPDH was used as a substrate (Fig. 6C, dashed line), further confirming that FeCN-induced electron leak only occurs when GP is oxidized on mGPDH and electrons are supplied into the enzyme.

All these experiments point towards CoQ binding site of mGPDH as the most likely source of the electron leak. To our knowledge, there is no specific inhibitor of CoQ site on mGPDH. We therefore tested effect of 2-n-heptyl-4-hydroxyquinoline N-oxide (HQNO), generalized competitive inhibitor, which binds to CoQ sites of various enzymes [38]. As shown in Fig. 7, in fully solubilized mitochondria (digitonin 6 g/g protein) blockade of mGPDH with 10 μM HQNO significantly decreases GP-dependent ROS production, while it has no effect on succinate-dependent ROS production, further implying that CoQ binding site is the source of electron leak on mGPDH.

3.4. mGPDH supercomplexes

Previous studies on isolation of mammalian mGPDH repeatedly observed a "holoenzyme" of 250–300 kDa consisting of only 75 kDa mGPDH protein suggesting oligomerization of this rather hydrophobic dehydrogenase. To search for different forms of the two dehydrogenases we analyzed digitonin solubilizates of mitochondrial membranes by means of native BN-PAGE and hrCN3-PAGE [26,28]. For detection we used WB with specific antibodies and in-gel activity staining (Fig. 8). We found mGPDH to be present in several homooligomeric forms, presumably as dimer, trimer and tetramer, as well as in high molecular mass supercomplex (SC) of more than 1000 kDa of yet unknown composition. The SC quantity was higher in hrCN3-PAGE judged both by WB (Fig. 8B) and in-gel activity (Fig. 8C), than in BN-PAGE (Fig. 8A) where

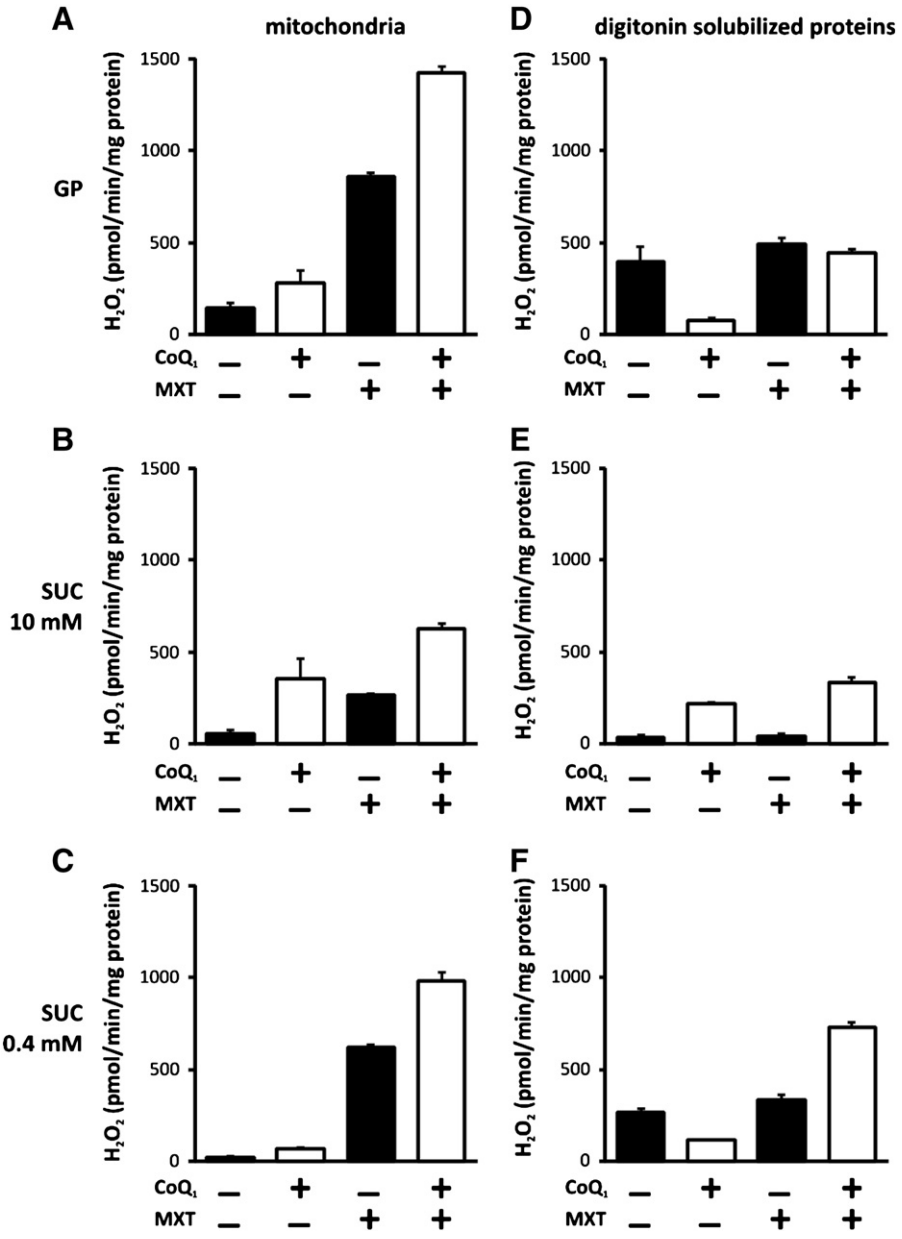

Fig. 4. Intactness of respiratory chain and CoQ influence ROS production. Data from Fig. 3 were redrawn to better document effect of decoupling dehydrogenase from complex III by solubilization on ROS production and its influence by CoQ_1. ROS production was detected in BAT mitochondria or 20,000 *g* digitonin solubilizates (6 g/g protein) with 10 mM glycerol-3-phosphate (GP), 10 mM succinate (SUC 10 mM) or 0.4 mM succinate (SUC 0.4 mM) respectively. Where indicated 1 μM myxothiazol (MXT) or 12 μM CoQ_1 (CoQ_1) was added into the assay. Results are mean ± SD from 3 to 6 replicates.

SC appeared as significantly fainter band and where monomer of mGPDH was observed as well. This indicates that this complex is labile and dissociates by the change of electrostatic interactions caused by the addition of Coomassie Blue dye. The content of mGPDH SC apparently declined with increasing concentration of digitonin and in turn, the contents of dimer and trimer increased correspondingly (Fig. 8C). In terms of the relative contribution of individual forms, dimer seems to be the most prominent form of mGPDH. Quantification of western signal gave the following relative values (dimer content set as 100%) for supercomplex:tetramer:trimer:dimer:monomer — 50:14:40:100:5 using hrCN3-PAGE and 25:17:51:100:42 using BN-PAGE and digitonin 2 g/g solubilizates. In the case of SDH only a 140 kDa monomer was found (not shown specifically but see western signal in Fig. 10).

To find out possible cross-reactions with other respiratory chain complexes we performed 2D electrophoretic analysis with the digitonin (2 g/g protein) solubilizates resolved by hrCN3-PAGE in the first dimension and by SDS-PAGE in the second. As seen in Fig. 9, individual forms of mGPDH were well resolved and even two distinct spots of mGPDH SC of >1 MDa could be seen (Fig. 9A), but none of them associated with signal of complex I, complex III or complex IV (Fig. 9B) i.e. OXPHOS complexes, which may share common electron transfer pathway with mGPDH and would therefore make kinetic sense. The putative mGPDH supercomplexes were smaller/larger than canonical respiratory chain SCs as can clearly be seen from the overlay of densitometric traces in Fig. 9C. As for the low molecular weight forms of mGPDH and their co-migration with the signal of other RC complexes, the patterns observed did not indicate association of mGPDH with assembled monomeric forms of respiratory chain complexes. Overlapping signals of mGPDH and SDH at 140 kDa apparently represent separate SDH monomers and mGPDH dimers because putative SDH–mGPDH heterodimer would have to have molecular weight of at least 210 kDa. With the antibody to Core2 subunit a significant signal was observed

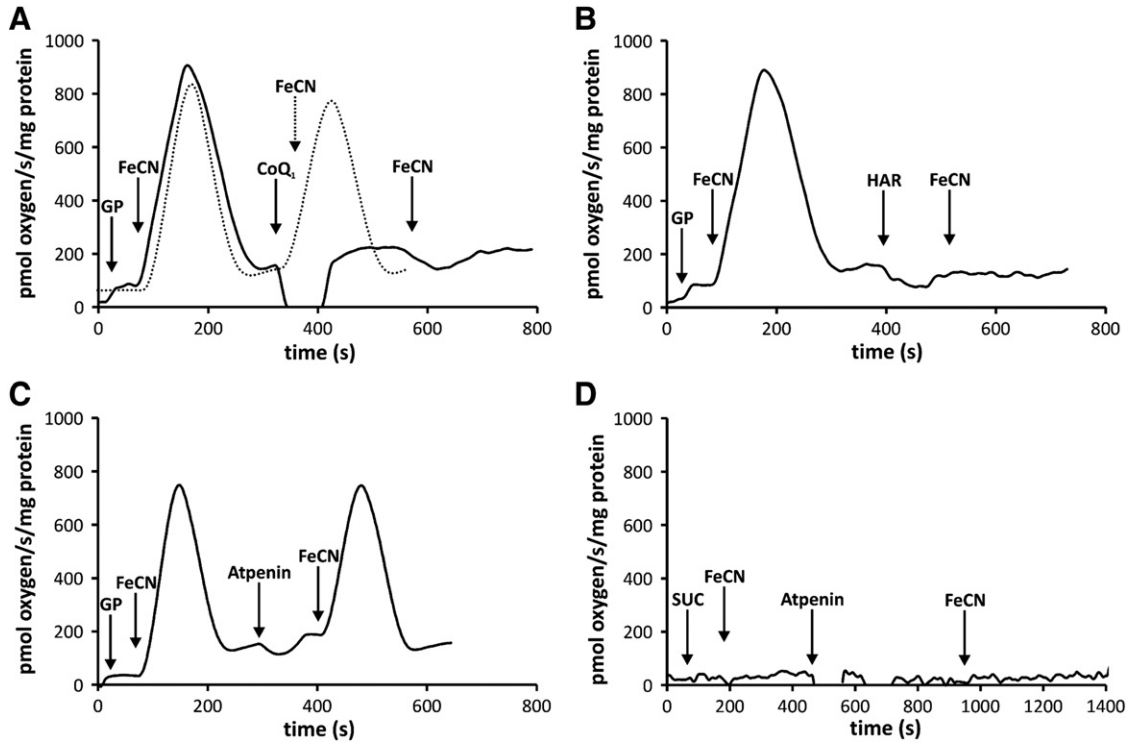

Fig. 5. Polarographic detection of ferricyanide-induced ROS production. ROS production was detected as ferricyanide (FeCN)-activated myxothiazol-insensitive oxygen uptake by digitonin solubilized BAT mitochondria (20,000 *g*, 2 g/g protein). (A,B) Coenzyme Q and hexaamine ruthenium (HAR) inhibit FeCN-induced ROS production by solubilized mGPDH determined as oxygen consumption with 10 mM glycerol-3-phosphate. At time intervals indicated in the graph, FeCN was added at a concentration of 62.5 μM. Addition of 16 μM CoQ_1 (A) or 125 μM HAR (B) completely abrogated FeCN-induced ROS production peak. Dotted line in (A) represents control trace with two subsequent additions of FeCN. (C) Addition of atpenin A5, inhibitor of SDH Q site does not have effect on GP-dependent, FeCN-induced ROS production. (D) FeCN induced ROS production is specific for mGPDH as there is no measurable myxothiazol-independent FeCN-induced ROS production if 0.4 mM succinate is used as substrate, and neither it is induced by the addition of atpenin A5. In each case representative measurement obtained independently with 2–5 different solubilizate preparations is shown.

in the region of 67 to 230 kDa but its profile was also different from that of mGPDH and most likely represents free Core2 subunit and assembly intermediates of complex III.

3.5. ROS production by the isolated enzyme

With the aim to analyze the ability to generate ROS by different soluble forms of mGPDH and SDH we set to develop protocol for in gel ROS measurements. Using this approach we were able to identify ROS production which co-localized with the WB signal detected by antibodies against mGPDH or SDH respectively (Fig. 10). ROS production was apparent in both dehydrogenases when soluble CoQ analog CoQ_1 was present, however, much higher intensity of ROS signal was again associated with mGPDH although the activity of mGPDH was 4-fold lower than that of SDH in the digitonin 2 g/g protein solubilizates used (see Fig. 2). ROS was thus detected in putative homooligomers as well as supercomplex form of mGPDH. In the absence of exogenous CoQ_1 only the signal of mGPDH-dependent ROS production was observed, mainly at mGPDH mono- and homooligomers. SDH ROS production without CoQ_1 was not observed with 0.4 mM succinate either (not shown), implicating that the isolated mGPDH but not SDH can generate ROS due to electron leak when supplied with the substrate only.

4. Discussion

In this paper we set to study ROS production by two flavin dehydrogenases of the mitochondrial respiratory chain — SDH and mGPDH in the system of frozen–thawed mitochondria solubilized with mild detergent digitonin. Solubilization of mitochondrial membranes with mild detergents is well established both for enzyme isolation and for the analysis of respiratory chain enzyme interactions in the membrane. Naturally, even this approach has its drawbacks. Solubilization may influence enzyme behavior as it is documented that enzyme activities of both SDH and especially mGPDH are affected by the lipid composition of the surrounding membrane. But on the other hand, it represents convenient option how to study dehydrogenases in isolation and dissect the portion of ROS production associated with enzymes themselves. It is well known that other complexes do contribute to overall ROS production from flavin dehydrogenases. This applies both for downstream complex III and for the upstream complex I or even complex II, which can be source of ROS through reverse electron transport from mGPDH. Solubilized enzymes thus offer unique opportunity to define *bona fide* sites of ROS production and to help with explanation of the mechanism of electron leak.

4.1. Solubilization and enzyme activities

As an experimental setup we chose to solubilize BAT mitochondria with increasing concentrations of digitonin and subsequently to fractionate them by centrifugation at 20,000 *g* for 20 min. This type of solubilization is widely used for the study of respiratory supercomplexes and has been shown to separate multiprotein complexes of up to 10 MDa [28,39]. To characterize conditions of solubilization we have first studied enzymatic activities in both solubilizates and sediments after solubilization. From these studies we can conclude that: (i) Only part of the mitochondrial proteins gets solubilized by detergent treatment (51–66% depending on digitonin concentration). Portion remains in the sediment and this does not change significantly by increasing detergent concentrations. (ii) Both mGPDH and SDH are partially inactivated by solubilization. As can be calculated from protein recoveries, at the highest digitonin concentration used (8 g/g protein), 53% of the protein was recovered in supernatant, but only 25.5% of GP:Q and 29.8% of succinate:Q activities

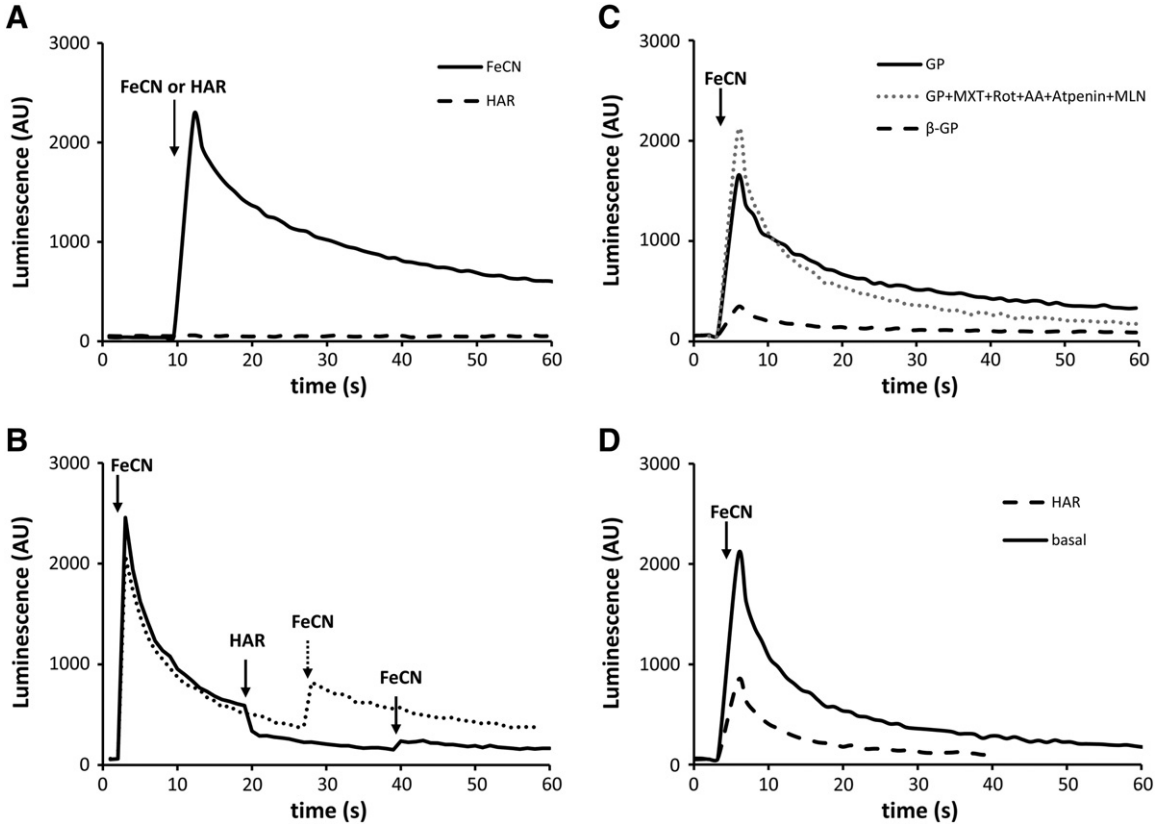

Fig. 6. Luminescence detection of ferricyanide-induced ROS production. ROS were detected as luminescence peak caused by the oxidation of luminol (1 mM) catalyzed by the HRP (2.5 U.mL^{-1}). ROS production was induced by FeCN (500 μM) or hexaamine ruthenium (HAR, 125 μM). 20,000 *g* solubilizates (digitonin 2 g/g protein) oxidizing 10 mM glycerol-3-phosphate were used. (A) While ferricyanide (FeCN, solid line) induces ROS production, hexaamine ruthenium (HAR, dashed line) cannot induce electron leak under identical conditions (n = 6). (B) HAR partially abrogates FeCN-induced ROS production if added sequentially to the same sample — solid line (n = 3). Dotted line represents control trace with two sequential additions of FeCN. (C) FeCN electron leak is mGPDH specific — does not depend on other complexes of respiratory chain. Solid line — control trace; dotted line — trace in the presence 1 μM rotenone (Rot), 1 μM myxothiazol (MXT), 1 mg.mL^{-1} antimycin A (AA), 1 μM atpenin A5, 10 mM malonate (MLN). It also cannot be induced when 10 mM non-oxidizable sn-glycerol-2-phosphate (β-GP) is used as a substrate — dashed line (n = 2). (D) HAR in the medium attenuates FeCN-induced ROS production. Solid line — no HAR present in the medium, dashed line — 125 μM HAR added to the incubation medium before measurement (n = 3). In each case representative measurement is shown and number of independent replicates from different solubilizate preparations is indicated as (n).

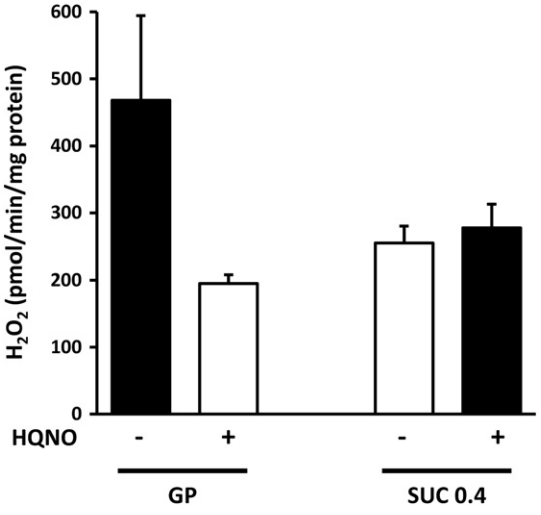

Fig. 7. HQNO inhibits GP-dependent ROS production. Hydrogen peroxide production was measured fluorometrically as oxidation of Amplex Red (50 μM) in the presence of HRP (1 U.mL^{-1}) in 20,000 *g* supernatants after solubilization of BAT mitochondria with digitonin (4 g/g protein). Either 10 mM glycerol-3-phosphate (GP) or 0.4 mM succinate (SUC 0.4) was used as substrates. Where indicated 10 μM 2-n-Heptyl-4-hydroxyquinoline N-oxide (HQNO) was used. Results are mean ± SD from 2 replicates.

were recovered. However, this inactivation is a well documented phenomenon, especially for mGPDH [33]. (iii) CoQ seems to be lost during solubilization, apparently more so in the case of SDH. This may be an indirect measure of enzyme affinity towards CoQ. Interestingly, low CoQ recovery during SDH purification has already been described [34]. In that study, SCCR activity could be reestablished by the addition of purified complex I, which retains CoQ during purification and thus served as CoQ source in the final preparation. In this context, the presence of CoQ observed in supercomplexes respiring on succinate [40] may not represent its direct association with SDH. (iv) At low digitonin concentration (1 g/g) we have observed the presence of patches of respiratory chain in the solubilizates, that contained at least flavin dehydrogenase (SDH, mGPDH) and complex III, as reported by the DH:cyt c activity. But based only on these measurements, they cannot be directly declared as respiratory supercomplexes. Furthermore, their content is low and above digitonin 4 g/g protein dehydrogenases become separated as individual entities without connection with the rest of OXPHOS. Apart from dehydrogenases and complex III, it is not clear, what are these complexes composed of (see below).

4.2. ROS production in solubilized mitochondria

In order to characterize ROS production by mGPDH and SDH we chose BAT mitochondria, that contain high (near equimolar) levels of both dehydrogenases [41]. Recently, several papers explored ROS production by flavin dehydrogenases, focusing on potential in vivo sources

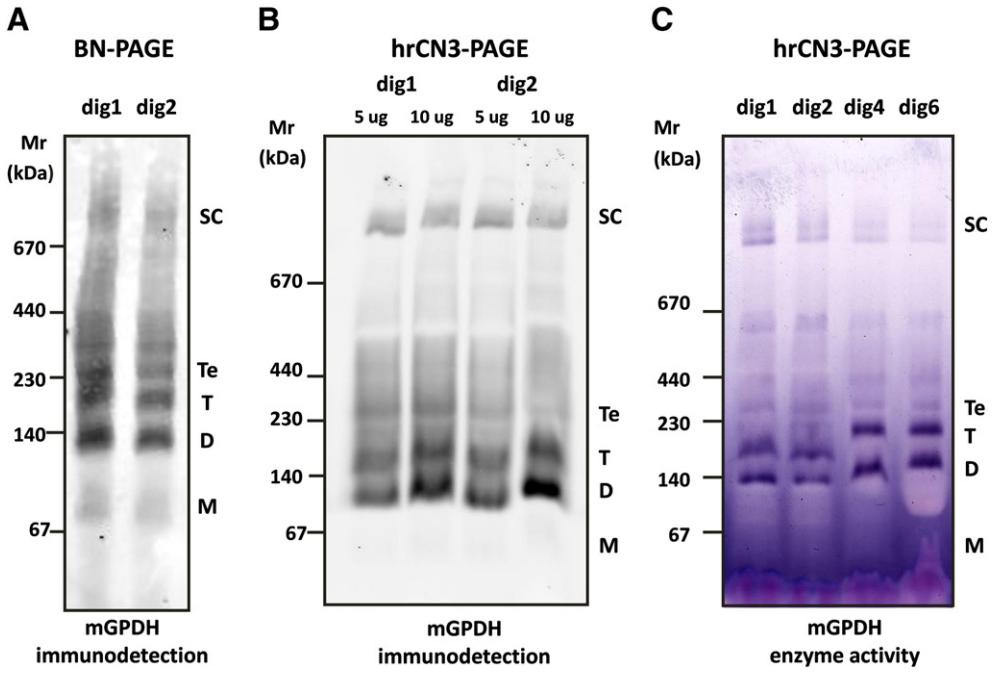

Fig. 8. Association of mGPDH into oligomeric complexes. BAT mitochondria were solubilized with different amounts of digitonin (dig) — 1, 2, 4 or 6 g/g protein. Solubilized proteins were separated using either BN-PAGE (A) or hrCN3-PAGE (B, C) native electrophoretic system (gel gradient 4–13%). (A, B) Western blot detection of mGPDH protein with specific antibody; (C) histochemical detection of mGPDH enzymatic activity using nitroblue tetrazolium as electron acceptor. mGPDH can be observed as faint monomer (M) band and in higher molecular mass complexes, presumably representing homodimer (D), homotrimer (T) homotetramer (Te) and high molecular mass supercomplex (SC) of unknown composition. Monomer was only visible, when BN-PAGE was used.

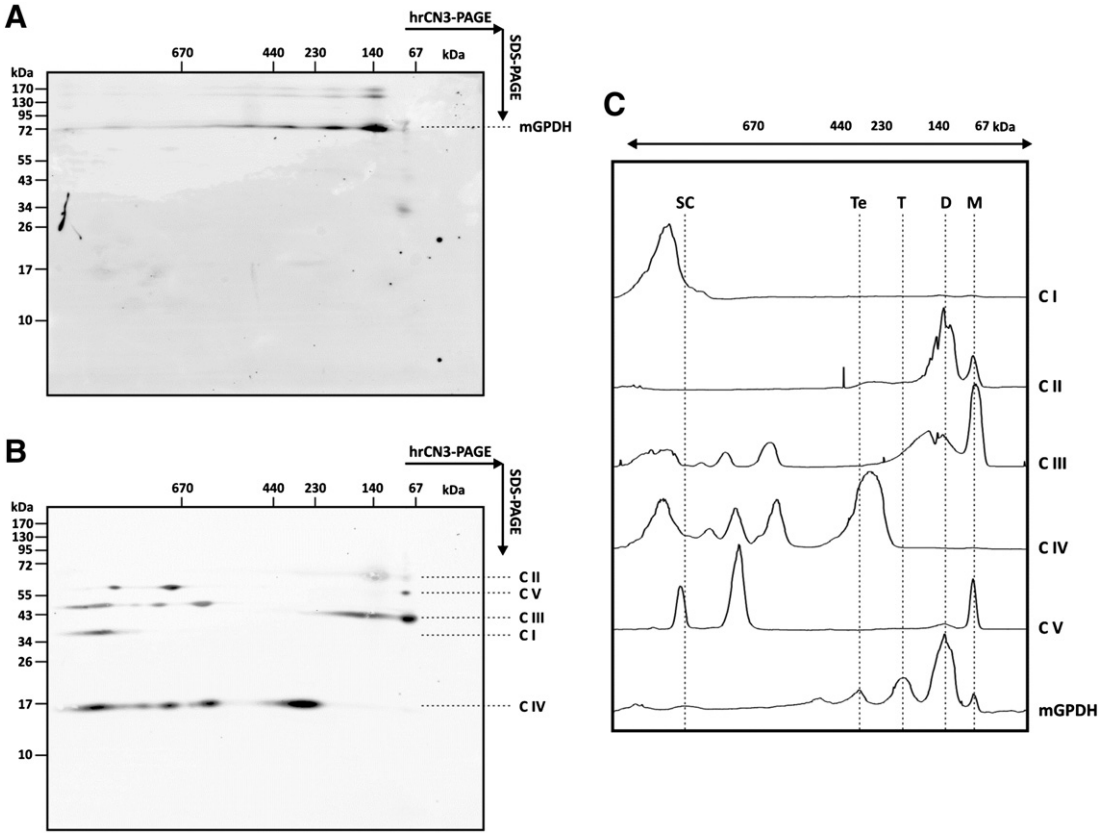

Fig. 9. 2D electrophoretic analysis of the association between mGPDH and OXPHOS complexes. Digitonin-solubilized mitochondrial proteins (2 g/g protein) were analyzed by two-dimensional hrCN3-PAGE/SDS-PAGE. After the first dimension separation by hrCN3-PAGE (50 μg protein), gel strip was treated with mercaptoethanol/SDS solution and SDS-PAGE was used in the second dimension followed by western blot analysis. (A) Detection of mGPDH protein. (B) Detection of OXPHOS subunits for individual respiratory chain complexes I–V: CI (NDUFA9), CII (SDHA), CIII (Core2), CIV (Cox4) and CV (α). (C) Profiles for 2D signal patterns of respective complexes. Position of mGPDH monomers (M), dimers (D), trimers (T), tetramers (Te) or supercomplexes (SC) is indicated.

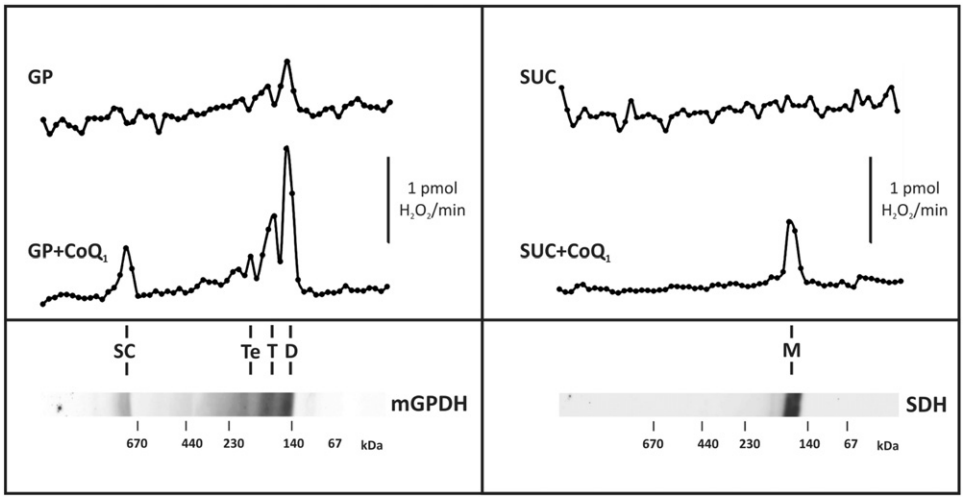

Fig. 10. Reactive oxygen species production by isolated enzyme. BAT mitochondria were solubilized with digitonin (2 g/g protein) and separated on hrCN3-PAGE. Part of the gel was used for western blot detection of mGPDH and SDH with specific antibodies (bottom panels). Gel strips were cut into 1 mm thick slices and those were used for fluorometric detection of ROS production with Amplex Red and HRP in the presence of substrate only (GP, SUC) or substrate and 12 μM CoQ_1 (GP + CoQ_1, SUC + CoQ_1). Representative traces from experiments performed on 3–6 independent preparations are shown; points on the curves represent actual measurements of ROS production in individual gel slices. M indicates monomer of SDH D, T, Te and SC indicate dimer, trimer, tetramer and supercomplex forms of mGPDH.

of ROS with succinate or GP as substrates [11,17,42]. While this analysis is important as well, due to the fact, that total in vivo ROS production with respective substrate will occur on several places in the OXPHOS, it may not provide an insight detailed enough to see into the mechanism on respective enzymes themselves. As our work focuses on solubilized mitochondria, we also chose to use frozen–thawed mitochondria as a control. Here we do not observe backflow towards complex I, which contributes to overall measured ROS levels [43].

Our data confirmed previous observations that SDH with saturating concentration of succinate (10 mM), produces very low quantities of ROS itself and most of the observed production happens on complex III [15]. Such ROS production diminishes after solubilization of the enzyme and points to low importance of electron leak from SDH under these conditions. More important are the observations with low succinate concentration (0.4 mM) and with GP. In both cases, the leak of electrons (ROS production) from respective dehydrogenase increases with increasing digitonin concentration. This clearly demonstrates that if electrons cannot be transferred further down the respiratory chain, both dehydrogenases tend to leak them towards O_2. As the dehydrogenases are fully soluble under high digitonin concentrations, it also demonstrates that such leak occurs on the respective enzymes themselves. In the case of SDH, this confirms recent observation made with the use of SDH inhibitor atpenin A5 [11,44]. As our system does not use inhibitors, it can serve as a further confirmation, that such ROS production really occurs on SDH and is not an artifact due to the presence of atpenin A5.

4.3. Effect of coenzyme Q

Because CoQ appeared to be depleted from solubilizates, we decided to check the effect of the addition of the soluble analog CoQ_1 on ROS production. For these experiments we used oxidized CoQ_1. While it was generally a pro-oxidant in mitochondrial preparations, it acted as an antioxidant in solubilized mitochondria with GP and 0.4 mM succinate. It most likely shows that reestablishment of electron flux by soluble CoQ_1 decreases pressure for electron leak from either mGPDH or SDH. As the antioxidant effect was abolished by MXT, it is clear that reoxidation of CoQ_1 on complex III is vital for its antioxidant role. Rather interesting is the strong prooxidant effect of reduced CoQ_1 (in the presence of MXT) with 0.4 mM succinate as substrate, because FAD should be the proposed site of electron leak here [11]. However, it has been shown that SDH activity is strongly regulated by the reduction state of CoQ pool and is highest with CoQ pool fully reduced [36]. Increase in the observed ROS production may therefore be also the effect of increased SDH enzymatic activity.

We further studied the potential of Q site as the source of electron leak by the use of one electron acceptors FeCN and HAR. The ability of ferricyanide to induce electron leak from mGPDH is well established [12,22]. Here we show that it is fully retained in solubilized mitochondria. Importantly, it cannot be inhibited by SDH inhibitor atpenin A5 or by complete inhibition of all other OXPHOS complexes but mGPDH. On the other hand, addition of the other single electron acceptor HAR (previously used in studies of complex I [45,46]) or CoQ abolishes the ability of FeCN to induce the leak of electrons. We do not have direct evidence of interaction sites for FeCN and HAR in case of mGPDH. In complex I, it was demonstrated, that FeCN displays ping–pong bi–bi kinetics [47], while HAR has ordered reaction mechanism [45]. It was interpreted so that FeCN interacts with FMN from the side of NADH binding cleft and HAR accepts electrons downstream of FMN. It is likely that FeCN interacts directly with FAD in mGPDH as well. mGPDH was proposed to have ping–pong reaction mechanism for GP reduction, analogously to the bacterial homolog GlpD [13,48]. FeCN would thus take one electron from $FADH_2$, producing flavin semiquinone, the actual source of ROS under these conditions. Most plausible explanation for the inhibitory effect of CoQ_1 and HAR on FeCN-induced electron leak is that they react downstream of FeCN reduction site (similarly to complex I) and channel electrons away from flavin semiquinone.

FeCN effect on SDH ROS production has not been demonstrated yet, despite the fact that SDH effectively transfers electrons to FeCN [49]. Here we show that neither solubilization, nor low succinate concentration or presence of atpenin A5 can induce FeCN-facilitated electron leak from SDH. It is rather surprising especially at low succinate concentrations, as it was suggested that incomplete substrate site occupancy is the prerequisite for ROS formation on SDH [11]. Empty substrate binding cleft with flavin semiquinone would represent rather likely place for one electron FeCN reduction, thus inducing electron leak, but this did not occur. All these demonstrate that transfer of electrons must be different between FAD and Q in both enzymes, with potential for channeling electrons away by single electron acceptor in the case of mGPDH.

Most direct evidence for CoQ site as the place of electron leak comes from experiments with HQNO. This generalized competitive inhibitor,

which binds to CoQ sites of various enzymes [38] has been found to bind also to bacterial mGPDH analog GlpD [48]. As the CoQ binding site is relatively conserved between GlpD and mGPDH, it is therefore conceivable to expect that it can interact with mGPDH as well. Interpretation of HQNO effect on GP-dependent ROS production is difficult in frozen thawed mitochondria, where inhibition of other CoQ sites in the respiratory chain, such as Q_o site of complex III, adds too much complexity. On the other hand, in fully solubilized mitochondria used in our experiment, its effect on GP-dependent ROS production should be specific for mGPDH only.

4.4. Mechanism of mGPDH dependent ROS production

This brings us to the question what is the exact mechanism of ROS production by mGPDH. Given its simple structure and most probable absence of FeS center, only the semiquinones formed at flavin or Q sites can be sources of electron leak. As discussed earlier, in SDH flavin has been proposed as the place of electron leak [11]. However, this does not seem to be the case with mGPDH. For this type of leak to occur in SDH, it is necessary that succinate concentrations are low and the substrate cleft displays only partial occupancy, thus allowing access of molecular oxygen to the flavin semiquinone intermediate formed and subsequent formation of superoxide. For mGPDH, ROS production increases linearly with increasing GP concentration at least to 40 mM, well past the Km for GP (2.9 mM) [43], which contradicts such possibility. Q site, or rather the CoQ semiquinone formed here, is therefore the most plausible source of electron leak on mGPDH. This is supported by our observations in this paper regarding interaction between CoQ and mGPDH as well as several lines of evidence in the literature.

(i) Structural evidence comes from the bacterial mGPDH analog GlpD, as there is no crystal structure available for the mammalian enzyme yet. However, the sequence is relatively well conserved between these proteins, as is the CoQ binding site. CoQ docking in GlpD occurs in the planar region oriented towards the lipid bilayer, which is analogous fold with another monotopic mitochondrial dehydrogenase — ETF:Q oxidase, which has also been shown to produce ROS [9,10,50]. On the contrary, SDH has a deep pocket with two binding sites for CoQ, which may represent natural protection against electron leak by the stabilization of ubisemiquinone radical formed during CoQ reduction [51,52]. Such stabilization seems to be essential in minimizing of the electron leak, as mutations in CoQ binding site of SDHC subunit were shown to increase ROS production [53].

(ii) It is also likely, that FAD semiquinone is only short lived and not present in the absence of GP in the substrate binding pocket. Yeh et al. proposed that it is most likely that catalysis occurs by ping–pong mechanism [48], meaning that fully reduced $FADH_2$ is produced by the oxidation of GP to dihydroxyacetone phosphate, which subsequently dissociates from the substrate binding pocket. Transfer of electrons to CoQ should then be concerted two electron process, but insufficient stabilization of semiquinone and its dissociation from the enzyme would result in electron leak. Analogous situation occurs in the presence of FeCN, where transfer of one electron from $FADH_2$ to FeCN leads to the formation of flavin semiquinone and formation of superoxide [12].

(iii) Another indirect evidence for CoQ as the source of electron leak in mGPDH comes from the observations of Brand's group, that superoxide is produced equally on both sides of the mitochondrial inner membrane [14,17]. FAD binding site is oriented towards intermembrane space and electrons leaking from this site would presumably be produced mostly towards intermembrane space as well.

4.5. mGPDH supercomplexes

Mitochondrial inner membrane is dense with average distance between protein complexes calculated to be only a few nanometers [54]. It is therefore not surprising that protein–protein interactions may occur. Their non-stochastic nature has been shown for example in the organization of oxidative phosphorylation apparatus. Here the theory of respiratory supercomplexes is widely accepted with individual OXPHOS complexes organized into higher molecular structures [40,55]. Among others it has been suggested that supercomplexes allow channeling of substrates between individual complexes and thus decrease the possibility of electron leak towards molecular oxygen and ROS production [56]. However, of the dehydrogenases communicating with CoQ pool, only complex I now represents an established part of OXPHOS supercomplex. Data on flavin dehydrogenases are scarcer and more controversial. They are absent in single particle electron microscopy studies of OXPHOS supercomplexes [57,58], but given their relatively small size they may simply be under the resolution limit of this technique. Neither kinetic studies of substrate channeling seem to support the presence of SDH in any supercomplex with complex III [56]. On the other hand at least some of the electrophoretic studies do detect SDH signal in high molecular weight complexes and could isolate other OXPHOS complexes by immunocapture via SDH antibody [40]. The same study also described respiratory competence of supercomplexes using succinate as substrate. There is also some support for mGPDH involvement in supercomplexes coming from yeast, where the mGPDH homolog Gut2p associates into “dehydrogenasome”, i.e. complex of several dehydrogenases supplying electrons to coenzyme Q [24].

It has also been clear since the early isolation experiments that mGPDH forms higher molecular weight aggregates, most likely due to its high hydrophobicity. During the purification by gel filtration the native mGPDH “holoenzyme” migrated at a molecular weight of approximately 250–300 kDa. As no other protein could be detected in this fraction, such complexes were considered to be homooligomeric aggregates [33].

Indeed, these homooligomeric structures were observed under native electrophoretic conditions of digitonin-solubilized BAT mitochondria. We were unsuccessful in determining any other interaction partners in these bands by crosslinking experiments and only mGPDH–mGPDH crosslinks were observed (not shown). It is therefore quite plausible that such homooligomers do represent native in vivo organization. It should also be noted that crystals of the bacterial mGPDH homolog GlpD also detect the native conformation to be a dimer and such dimerization seems to be determined by large hydrophobic areas present on the surface of the protein not buried into the membrane [48]. However, this does not explain the molecular nature of the observed approximately 1 MDa mGPDH supercomplex. Its partial dissociation after Coomassie dye addition points more towards weak electrostatic interactions than to hydrophobic interface which is likely in the homooligomers. As it does not co-migrate with OXPHOS complexes on 2D gels, it most likely does not represent “OXPHOS supercomplex” in the traditional sense. Our experiments also indicate that ROS production by the supercomplex form of the enzyme is broadly in par with the relative content of individual forms of mGPDH. Therefore such structure does not seem to be any better in channeling electrons towards complex III and thus preventing ROS production. We do not know molecular nature of this complex yet, but one speculation based on yeast gut2p may be, that such complex represents association of several flavin dehydrogenases such as mGPDH and ETF:Q oxidoreductase.

4.6. Isolated mGPDH as an ROS producer

Last, we have also demonstrated, that both isolated mGPDH and SDH are capable of ROS production. While mGPDH can do so in the absence of exogenous CoQ, SDH can produce ROS only, if exogenous CoQ was present. This is presumably in agreement with our observations that SDH is preferentially depleted of CoQ during solubilization. It has been demonstrated, that partially purified mGPDH did produce FeCN-dependent ROS [12]. However, this is the first direct confirmation, that both dehydrogenases can be independent sources of ROS and this does not occur only indirectly on other OXPHOS complexes. We have

also demonstrated that all native forms of mGPDH — homooligomers as well as its supercomplex form do produce ROS. It would be interesting to judge, whether association on mGPDH into supercomplex structures reduces ROS production. Although majority of ROS were produced by lower molecular forms it is difficult to make such conclusions. ROS detection in gel is merely semiquantitative and thus it is hard to correlate its intensity with the native western signal.

Taken together, in this paper we studied mechanisms of ROS production by two mitochondrial flavin dehydrogenases mGPDH and SDH. While we confirmed flavin as the most likely source of electron leak in SDH, we propose coenzyme Q as the site of ROS production in the case of mGPDH. Furthermore, using native electrophoretic systems, we demonstrated that mGPDH associates into homooligomers as well as high molecular weight supercomplexes, which represent native forms of mGPDH in the membrane. In the end, we also demonstrated that isolated mGPDH itself as well as its supramolecular assemblies are all capable of ROS production.

Supplementary data to this article can be found online at http://dx.doi.org/10.1016/j.bbabio.2013.08.007.

Acknowledgements

This work was supported by Grant Agency of the Czech Republic (P303/10/P227), Ministry of Education, Youth and Sports of the Czech Republic (ERC CZ LL1204 and RVO 67985823) and Grant Agency of the Charles University (750213).

References

[1] B. Halliwell, J. Gutteridge, Free Radicals in Biology and Medicine, Third ed. Oxford University Press, Oxford, 1999.
[2] S.G. Rhee, Cell signaling. H_2O_2, a necessary evil for cell signaling, Science 312 (2006) 1882–1883.
[3] A. Boveris, N. Oshino, B. Chance, The cellular production of hydrogen peroxide, Biochem. J. 128 (1972) 617–630.
[4] G. Loschen, L. Flohe, B. Chance, Respiratory chain linked H(2)O(2) production in pigeon heart mitochondria, FEBS Lett. 18 (1971) 261–264.
[5] E. Cadenas, K.J. Davies, Mitochondrial free radical generation, oxidative stress, and aging, Free Radic. Biol. Med. 29 (2000) 222–230.
[6] Q. Chen, E.J. Vazquez, S. Moghaddas, C.L. Hoppel, E.J. Lesnefsky, Production of reactive oxygen species by mitochondria: central role of complex III, J. Biol. Chem. 278 (2003) 36027–36031.
[7] A.V. Kareyeva, V.G. Grivennikova, G. Cecchini, A.D. Vinogradov, Molecular identification of the enzyme responsible for the mitochondrial NADH-supported ammonium-dependent hydrogen peroxide production, FEBS Lett. 585 (2011) 385–389.
[8] L. Tretter, V. Adam-Vizi, Generation of reactive oxygen species in the reaction catalyzed by alpha-ketoglutarate dehydrogenase, J. Neurosci. 24 (2004) 7771–7778.
[9] E.L. Seifert, C. Estey, J.Y. Xuan, M.E. Harper, Electron transport chain-dependent and -independent mechanisms of mitochondrial H_2O_2 emission during long-chain fatty acid oxidation, J. Biol. Chem. 285 (2010) 5748–5758.
[10] P. Schonfeld, L. Wojtczak, Brown adipose tissue mitochondria oxidizing fatty acids generate high levels of reactive oxygen species irrespective of the uncoupling protein-1 activity state, Biochim. Biophys. Acta 1817 (2012) 410–418.
[11] C.L. Quinlan, A.L. Orr, I.V. Perevoshchikova, J.R. Treberg, B.A. Ackrell, M.D. Brand, Mitochondrial complex II can generate reactive oxygen species at high rates in both the forward and reverse reactions, J. Biol. Chem. 287 (2012) 27255–27264.
[12] Z. Drahota, S.K. Chowdhury, D. Floryk, T. Mracek, J. Wilhelm, H. Rauchova, G. Lenaz, J. Houstek, Glycerophosphate-dependent hydrogen peroxide production by brown adipose tissue mitochondria and its activation by ferricyanide, J. Bioenerg. Biomembr. 34 (2002) 105–113.
[13] T. Mracek, Z. Drahota, J. Houstek, The function and the role of the mitochondrial glycerol-3-phosphate dehydrogenase in mammalian tissues, Biochim. Biophys. Acta 1827 (2013) 401–410.
[14] S. Miwa, M.D. Brand, The topology of superoxide production by complex III and glycerol 3-phosphate dehydrogenase in *Drosophila* mitochondria, Biochim. Biophys. Acta 1709 (2005) 214–219.
[15] M. Vrbacky, Z. Drahota, T. Mracek, A. Vojtiskova, P. Jesina, P. Stopka, J. Houstek, Respiratory chain components involved in the glycerophosphate dehydrogenase-dependent ROS production by brown adipose tissue mitochondria, Biochim. Biophys. Acta 1767 (2007) 989–997.
[16] T. Mracek, A. Pecinova, M. Vrbacky, Z. Drahota, J. Houstek, High efficiency of ROS production by glycerophosphate dehydrogenase in mammalian mitochondria, Arch. Biochem. Biophys. 481 (2009) 30–36.
[17] A.L. Orr, C.L. Quinlan, I.V. Perevoshchikova, M.D. Brand, A refined analysis of superoxide production by mitochondrial sn-glycerol 3-phosphate dehydrogenase, J. Biol. Chem. 287 (2012) 42921–42935.
[18] F. Sun, X. Huo, Y. Zhai, A. Wang, J. Xu, D. Su, M. Bartlam, Z. Rao, Crystal structure of mitochondrial respiratory membrane protein complex II, Cell 121 (2005) 1043–1057.
[19] F.L. Muller, Y. Liu, M.A. Abdul-Ghani, M.S. Lustgarten, A. Bhattacharya, Y.C. Jang, H. Van Remmen, High rates of superoxide production in skeletal-muscle mitochondria respiring on both complex I- and complex II-linked substrates, Biochem. J. 409 (2008) 491–499.
[20] M.A. Selak, S.M. Armour, E.D. MacKenzie, H. Boulahbel, D.G. Watson, K.D. Mansfield, Y. Pan, M.C. Simon, C.B. Thompson, E. Gottlieb, Succinate links TCA cycle dysfunction to oncogenesis by inhibiting HIF-alpha prolyl hydroxylase, Cancer Cell 7 (2005) 77–85.
[21] M. Jain, R. Nilsson, S. Sharma, N. Madhusudhan, T. Kitami, A.L. Souza, R. Kafri, M.W. Kirschner, C.B. Clish, V.K. Mootha, Metabolite profiling identifies a key role for glycine in rapid cancer cell proliferation, Science 336 (2012) 1040–1044.
[22] Z. Drahota, H. Rauchova, P. Jesina, A. Vojtiskova, J. Houstek, Glycerophosphate-dependent peroxide production by brown fat mitochondria from newborn rats, Gen. Physiol. Biophys. 22 (2003) 93–102.
[23] P.M. Sousa, S.T. Silva, B.L. Hood, N. Charro, J.N. Carita, F. Vaz, D. Penque, T.P. Conrads, A.M. Melo, Supramolecular organizations in the aerobic respiratory chain of *Escherichia coli*, Biochimie 93 (2011) 418–425.
[24] X. Grandier-Vazeille, K. Bathany, S. Chaignepain, N. Camougrand, S. Manon, J.M. Schmitter, Yeast mitochondrial dehydrogenases are associated in a supramolecular complex, Biochemistry 40 (2001) 9758–9769.
[25] B. Cannon, O. Lindberg, Mitochondria from brown adipose tissue: isolation and properties, Methods Enzymol. 55 (1979) 65–78.
[26] I. Wittig, M. Karas, H. Schagger, High resolution clear native electrophoresis for in-gel functional assays and fluorescence studies of membrane protein complexes, Mol Cell Proteomics 6 (2007) 1215–1225.
[27] J. Wilhelm, V. Vilim, Variables in xanthine oxidase-initiated luminol chemiluminescence: implications for chemiluminescence measurements in biological systems, Anal. Biochem. 158 (1986) 201–210.
[28] I. Wittig, H.P. Braun, H. Schagger, Blue native PAGE, Nat. Protoc. 1 (2006) 418–428.
[29] H. Schagger, G. von Jagow, Tricine-sodium dodecyl sulfate-polyacrylamide gel electrophoresis for the separation of proteins in the range from 1 to 100 kDa, Anal. Biochem. 166 (1987) 368–379.
[30] T. Mracek, P. Jesina, P. Krivakova, R. Bolehovska, Z. Cervinkova, Z. Drahota, J. Houstek, Time-course of hormonal induction of mitochondrial glycerophosphate dehydrogenase biogenesis in rat liver, Biochim. Biophys. Acta 1726 (2005) 217–223.
[31] W.M. Frederiks, F. Marx, G.L. Myagkaya, A histochemical study of changes in mitochondrial enzyme activities of rat liver after ischemia in vitro, Virchows Arch B Cell Pathol Incl Mol Pathol 51 (1986) 321–329.
[32] L. Yu, C.A. Yu, Quantitative resolution of succinate–cytochrome c reductase into succinate–ubiquinone and ubiquinol–cytochrome c reductases, J. Biol. Chem. 257 (1982) 2016–2021.
[33] I.R. Cottingham, C.I. Ragan, Purification and properties of L-3-glycerophosphate dehydrogenase from pig brain mitochondria, Biochem. J. 192 (1980) 9–18.
[34] Y. Hatefi, A.G. Haavik, L.R. Fowler, D.E. Griffiths, Studies on the electron transfer system. XLII. Reconstitution of the electron transfer system, J. Biol. Chem. 237 (1962) 2661–2669.
[35] B.A. Ackrell, E.B. Kearney, T.P. Singer, Mammalian succinate dehydrogenase, Methods Enzymol. 53 (1978) 466–483.
[36] M. Gutman, E.B. Kearney, T.P. Singer, Control of succinate dehydrogenase in mitochondria, Biochemistry 10 (1971) 4763–4770.
[37] M. Gutman, E.B. Kearney, T.P. Singer, Regulation of succinate dehydrogenase activity by reduced coenzymes Q10, Biochemistry 10 (1971) 2726–2733.
[38] M. Kogut, J.W. Lightbown, Selective inhibition by 2-heptyl-4-hydroxyquinoline N-oxide of certain oxidation-reduction reactions, Biochem. J. 84 (1962) 368–382.
[39] V. Strecker, Z. Wumaier, I. Wittig, H. Schagger, Large pore gels to separate mega protein complexes larger than 10 MDa by blue native electrophoresis: isolation of putative respiratory strings or patches, Proteomics 10 (2010) 3379–3387.
[40] R. Acin-Perez, P. Fernandez-Silva, M.L. Peleato, A. Perez-Martos, J.A. Enriquez, Respiratory active mitochondrial supercomplexes, Mol Cell 32 (2008) 529–539.
[41] J. Houstek, B. Cannon, O. Lindberg, Gylcerol-3-phosphate shuttle and its function in intermediary metabolism of hamster brown-adipose tissue, Eur. J. Biochem. 54 (1975) 11–18.
[42] L. Tretter, V. Adam-Vizi, High Ca^{2+} load promotes hydrogen peroxide generation via activation of alpha-glycerophosphate dehydrogenase in brain mitochondria, Free Radic. Biol. Med. 53 (2012) 2119–2130.
[43] L. Tretter, K. Takacs, V. Hegedus, V. Adam-Vizi, Characteristics of alpha-glycerophosphate-evoked H_2O_2 generation in brain mitochondria, J. Neurochem. 100 (2007) 650–663.
[44] I. Siebels, S. Drose, Q-site inhibitor induced ROS production of mitochondrial complex II is attenuated by TCA cycle dicarboxylates, Biochim. Biophys. Acta 1827 (2013) 1156–1164.
[45] V.D. Sled, A.D. Vinogradov, Kinetics of the mitochondrial NADH-ubiquinone oxidoreductase interaction with hexammineruthenium(III), Biochim. Biophys. Acta 1141 (1993) 262–268.
[46] A.D. Vinogradov, NADH/NAD+ interaction with NADH: ubiquinone oxidoreductase (complex I), Biochim. Biophys. Acta 1777 (2008) 729–734.
[47] G. Dooijewaard, E.C. Slater, Steady-state kinetics of high molecular weight (type-I) NADH dehydrogenase, Biochim. Biophys. Acta 440 (1976) 1–15.
[48] J.I. Yeh, U. Chinte, S. Du, Structure of glycerol-3-phosphate dehydrogenase, an essential monotopic membrane enzyme involved in respiration and metabolism, Proc. Natl. Acad. Sci. U. S. A. 105 (2008) 3280–3285.
[49] A.D. Vinogradov, E.V. Gavrikova, V.G. Goloveshkina, A new ferricyanide reactive site in soluble succinate dehydrogenase, Biochem. Biophys. Res. Commun. 65 (1975) 1264–1269.

[50] J. Zhang, F.E. Frerman, J.J. Kim, Structure of electron transfer flavoprotein-ubiquinone oxidoreductase and electron transfer to the mitochondrial ubiquinone pool, Proc. Natl. Acad. Sci. U. S. A. 103 (2006) 16212–16217.
[51] R. Horsefield, V. Yankovskaya, G. Sexton, W. Whittingham, K. Shiomi, S. Omura, B. Byrne, G. Cecchini, S. Iwata, Structural and computational analysis of the quinone-binding site of complex II (succinate-ubiquinone oxidoreductase): a mechanism of electron transfer and proton conduction during ubiquinone reduction, J. Biol. Chem. 281 (2006) 7309–7316.
[52] C.A. Yu, S. Nagaoka, L. Yu, T.E. King, Evidence for the existence of a ubiquinone protein and its radical in the cytochromes b and c1 region in the mitochondrial electron transport chain, Biochem. Biophys. Res. Commun. 82 (1978) 1070–1078.
[53] B.G. Slane, N. Aykin-Burns, B.J. Smith, A.L. Kalen, P.C. Goswami, F.E. Domann, D.R. Spitz, Mutation of succinate dehydrogenase subunit C results in increased O2.-, oxidative stress, and genomic instability, Cancer Res. 66 (2006) 7615–7620.
[54] G. Lenaz, M.L. Genova, Structure and organization of mitochondrial respiratory complexes: a new understanding of an old subject, Antioxid Redox Signal 12 (2010) 961–1008.
[55] H. Schagger, Respiratory chain supercomplexes of mitochondria and bacteria, Biochim. Biophys. Acta 1555 (2002) 154–159.
[56] G. Lenaz, M.L. Genova, Supramolecular organisation of the mitochondrial respiratory chain: a new challenge for the mechanism and control of oxidative phosphorylation, Adv Exp Med Biol 748 (2012) 107–144.
[57] N.V. Dudkina, M. Kudryashev, H. Stahlberg, E.J. Boekema, Interaction of complexes I, III, and IV within the bovine respirasome by single particle cryoelectron tomography, Proc Natl Acad Sci U S A 108 (2011) 15196–15200.
[58] N.V. Dudkina, H. Eubel, W. Keegstra, E.J. Boekema, H.P. Braun, Structure of a mitochondrial supercomplex formed by respiratory-chain complexes I and III, Proc. Natl. Acad. Sci. U. S. A. 102 (2005) 3225–3229.